JCEC
THE JOURNAL OF ENGINEERING AND EXACT SCIENCES

OPEN ACCESS

The Journal of Engineering and Exact Sciences – jCEC, Vol. 09 N. 01 (2023)
journal homepage: https://periodicos.ufv.br/jcec
eISSN: 2527-1075
ISSN: 2446-9416

Finite element simulations of auxetic structure combined with honeycomb using unidirectional continuous carbon fiber composite properties

Simulações de elementos finitos de estrutura auxética combinada com honeycomb utilizando propriedades de compósito de fibras de carbono contínuas e unidirecionais

Article Info:
Article history: Received 2023-01-01 / Accepted 2023-02-20 / Available online 2023-02-20
doi: 10.18540/jcecvl9iss1pp15430-01e

Nathália Mello Mascarenhas Paixão
ORCID: https://orcid.org/0000-0003-0869-8258
Centro Federal de Educação Tecnológica de Minas Gerais e Universidade Federal de Minas Gerais, Brazil
E-mail: nathaliamello@cefetmg.br
Antônio Ferreira Ávila
ORCID: https://orcid.org/0000-0003-4788-8943
Universidade Federal de Minas Gerais, Brazil
E-mail: avila@demec.ufmg.br

Resumo
Os metamateriais têm sido estudados ao longo das últimas décadas, uma vez que podem apresentar um comportamento mecânico peculiar. Um exemplo é a estrutura auxética re-entrante, que pode exibir um coeficiente de Poisson negativo. Do mesmo modo, a estrutura *honeycomb* também tem sido amplamente utilizada, principalmente em painéis sanduíche. Apesar de vários estudos incluindo estas geometrias, a utilização do compósito como matéria-prima não tem sido relatada na literatura, portanto, este trabalho visou realizar simulações de elementos finitos de estruturas celulares formadas por geometrias *honeycomb* combinada com auxética re-entrante, utilizando propriedades de compósito de fibra de carbono contínua e unidirecional em matriz epóxi. Para tal, foram utilizados três tipos de modelagens: viga, casca e sólido e foram aplicados dois conjuntos de restrições para cada modelo. Ao analisar os perfis de deformação total obtidos para estes três modelos, foi possível observar que tanto a modelagem de viga como a modelagem de casca promoveram resultados próximos à modelagem tridimensional ao aplicar um deslocamento de compressão vertical, sendo que a modelagem de viga mostrou uma melhor aproximação. Por outro lado, ao aplicar o deslocamento de compressão horizontalmente, a modelagem de viga mostrou-se inadequada, enquanto que a modelagem de casca apresentou valores próximos do modelo tridimensional. Portanto, conclui-se que é possível modelar estruturas semelhantes utilizando elemento de casca em vez de elemento tridimensional.
Palavras-chave: Materiais compósitos. Compósito de fibra de carbono com epóxi. Simulação de elementos finitos. Metamaterial. Estrutura auxética.

Abstract
Metamaterials have been studied over the last few decades, as they may exhibit peculiar mechanical behavior. An example is the re-entrant auxetic structure, which can display negative Poisson ratio. Likewise, the honeycomb structure has also been widely used, mainly in sandwich-panels. Despite several studies including these geometries, the use of composite as raw material has not been reported in the literature, so this work aimed to perform finite element simulations of combined honeycomb and re-entrant auxetic structures using properties of continuous, unidirectional carbon fiber composite in epoxy matrix. For this, three types of modeling were used: beam, shell and solid and two sets of constraints were applied for each model. By analyzing the total deformation profiles

obtained for these three models, it was possible to observe that both beam and shell modeling results were close to the three-dimensional modeling when applying a vertical compression displacement, in which beam modeling showed a better approximation. On the other hand, when applying the compression displacement horizontally, the beam modeling proved to be inadequate, while the shell modeling presented values close to the solid modeling. Therefore, it is concluded that it is possible to model similar structures using shell element instead of solid element.
Keywords: Composite materials. Carbon fiber epoxy composite. Finite element simulation. Metamaterial. Auxetic structure.

1. Introduction

Metamaterials have been widely studied over the last few decades, as they can display peculiar mechanical behavior that a continuous isotropic material would hardly show (Zhong *et al*., 2019). Examples of cellular materials are the re-entrant auxetic and the honeycomb structures (Masters and Evans, 1996), which can be seen in Figure 1. The honeycomb geometry is used as a core in composite materials of sandwich-panels, increasing its flexural rigidity, allowing mass reduction due to void spaces (Chen *et al*., 2011; Crupi *et al*., 2012). The re-entrant auxetic geometry is an adaptation of honeycomb and leads to a negative Poisson ratio (Wang *et al*., 2018).

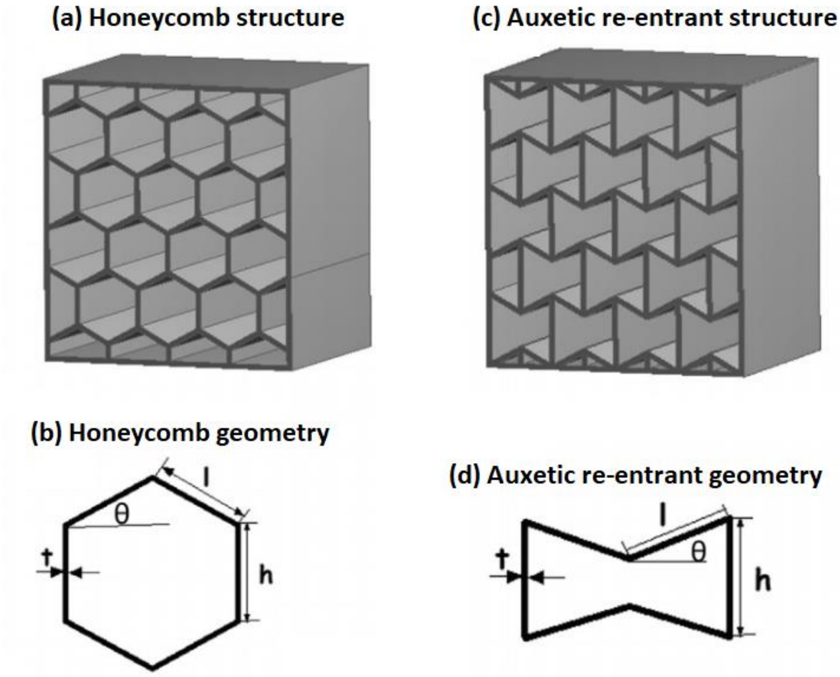

Figure 1 – Honeycomb and re-entrant auxetic structures and geometries. (Adapted from Shruti *et al*., 2021)

It has already been reported simulations and experimental setups using a combination of auxetic and honeycomb geometries, in which the raw material was an isotropic polymer (Shruti *et al*., 2021; Xu *et al*., 2019). A lot of geometries of metamaterials were also simulated and experimentally studied (Fei at al., 2020; Wang *et al*., 2019; Karathanasopoulos *et al*., 2018; Mousanezhad *et al*., 2016), however the manufacture of this specific geometry – re-entrant auxetic combined with honeycomb – using composite as raw material has not yet been reported in the literature. Therefore, this work proposed to carry out finite element simulations of a structure formed by a combination of honeycomb and auxetic geometries, using properties of a composite material of unidirectional carbon fibers in a thermoset epoxy polymer matrix.

Composite materials are formed by two or more distinct insoluble phases with a well-defined interface. Its advantages are the obtainment of a material that has properties resulted from the phase combinations, in which no single material is capable to display (Daniel and Ishai, 2006). In the case of composites made of continuous and unidirectional fibers, study object of this work, the properties such as Young's modulus and mechanical strength are higher along fibers direction, while in the other two directions the properties are equal. This type of material is also called orthotropic, as it has three planes of symmetry (Jones, 1990).

2. Simulations methodology

Six finite element simulations were performed using the commercial software *Ansys Workbench*. Simulations were carried out with three distinct elements and models: one-dimensional (using beam element), using a two-dimensional shell element and using a three-dimensional volumetric element (solid). For each of these three models, two simulations were performed, varying only the constraints of the structures from one situation to the other. The following topics refer, respectively, to the raw material used, the geometries for the three models, the meshing generation and the constraints of the models. Figure 2 presents a flowchart in which it is possible to see a summary of the steps of this methodology.

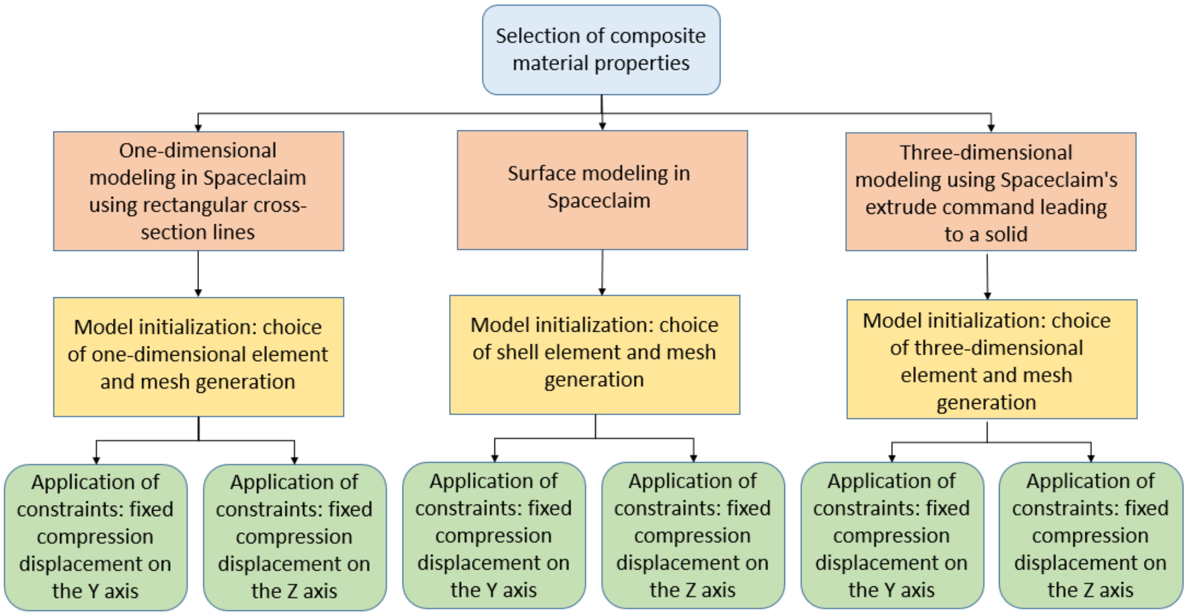

Figure 2 – Flowchart showing simulation steps.

2.1 Material Properties

In all simulations, the properties of a composite material of continuous and unidirectional carbon fibers in an epoxy polymer matrix were used. The mechanical properties considered were in the database of the *Ansys* software, whose material is named *Epoxy Carbon UD (230 GPa) Prepreg.* In all simulations the fiber direction was aligned with *X* direction of the geometries, which corresponds to the dimension where the thickness of the structures lies through.

2.2 Geometry Modeling

All geometry models were built in *Spaceclaim* included in *Ansys Workbench*. The structures were modeled with 10mm thickness, two unit cells on the horizontal *Z*-axis and five stacked lines.

Figures 3, 4 and 5 show the front and isometric views of the three different models: one-dimensional (beam element), surfaces (shell element) and three-dimensional (solid element), respectively.

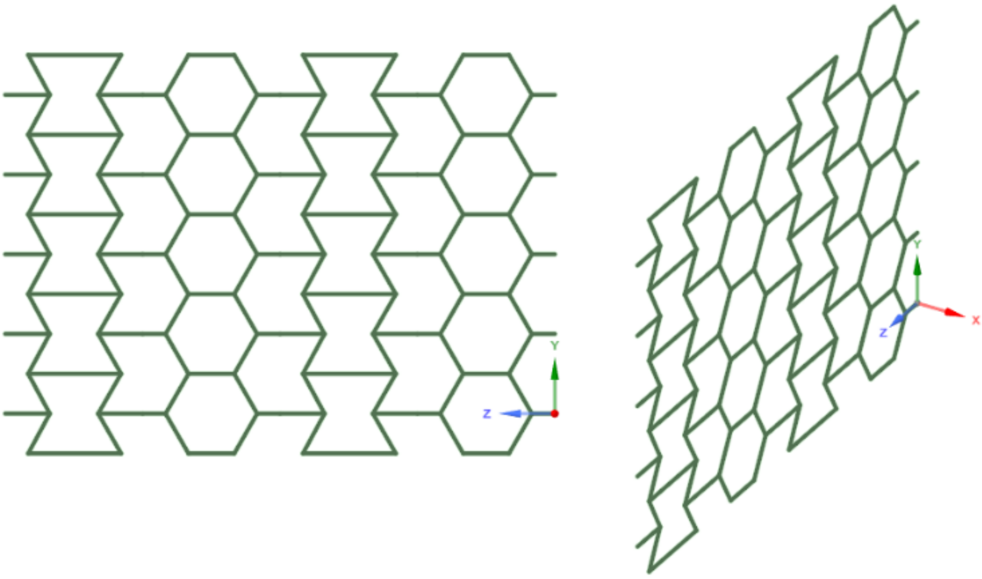

Figure 3 – Frontal and isometric views of geometry generated in *Spaceclaim* used to perform simulations of one-dimensional elements.

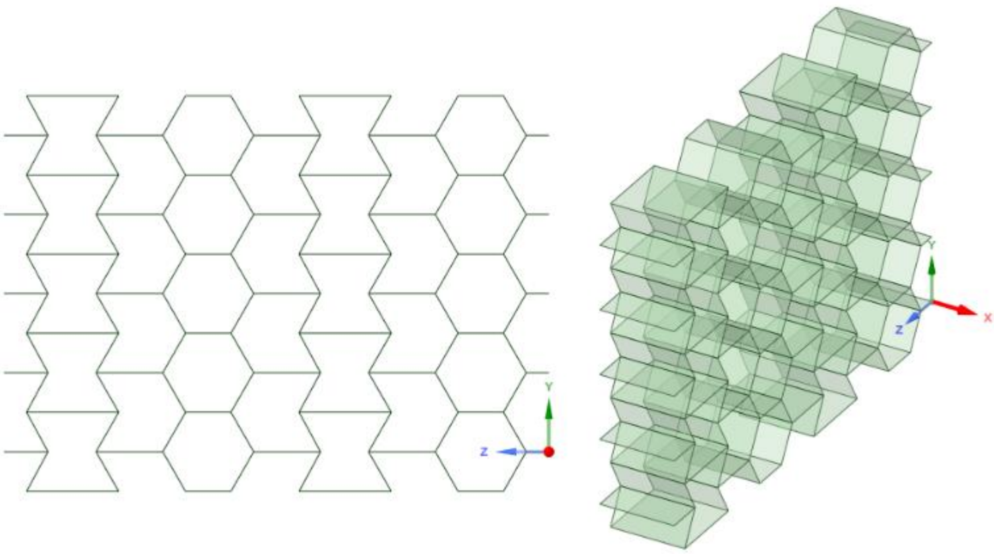

Figure 4 – Frontal and isometric views of geometry generated in *Spaceclaim* used to perform simulations of two-dimensional elements (shell).

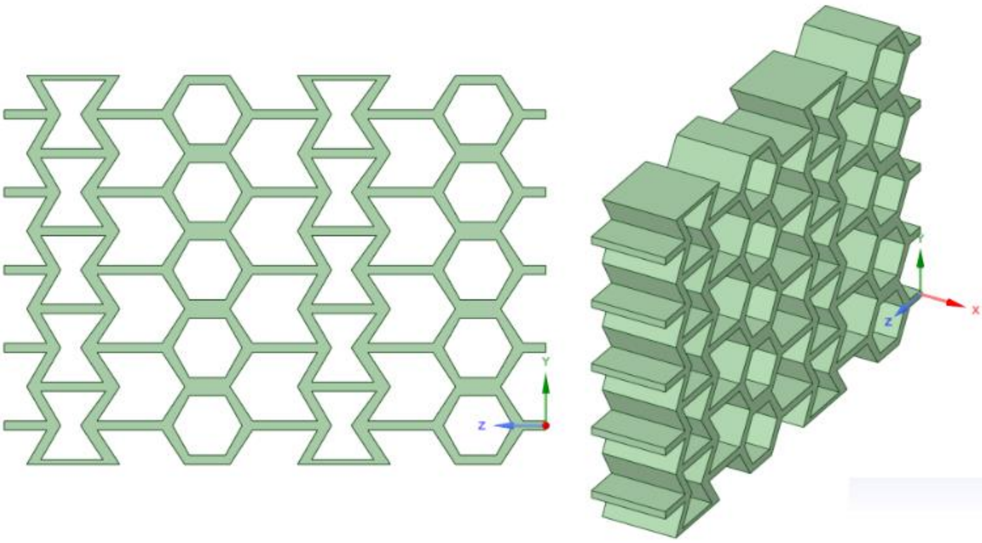

Figure 5 – Frontal and isometric views of geometry generated in *Spaceclaim* used to perform simulations of three-dimensional elements (solid body).

2.3 Mesh Generation

For the three models, 2mm long elements were used and the mesh was automatically generated by the software. Figures 6, 7 and 8 show, respectively, frontal and isometric views of the models after meshing generation of one-dimensional (beam), shell and three-dimensional (solid) models.

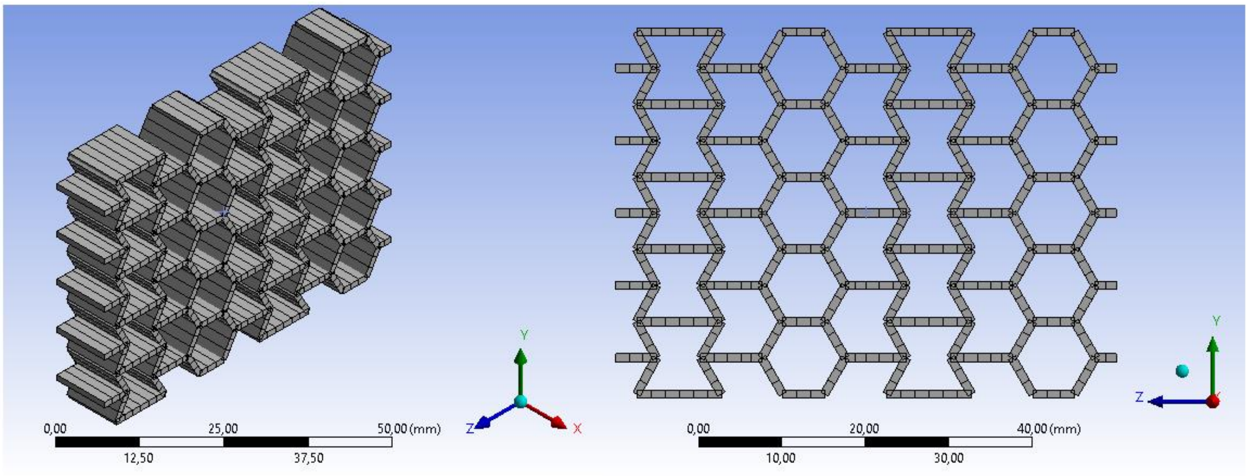

Figure 6 – Frontal and isometric views of model meshing used for simulation of one-dimensional elements (beam).

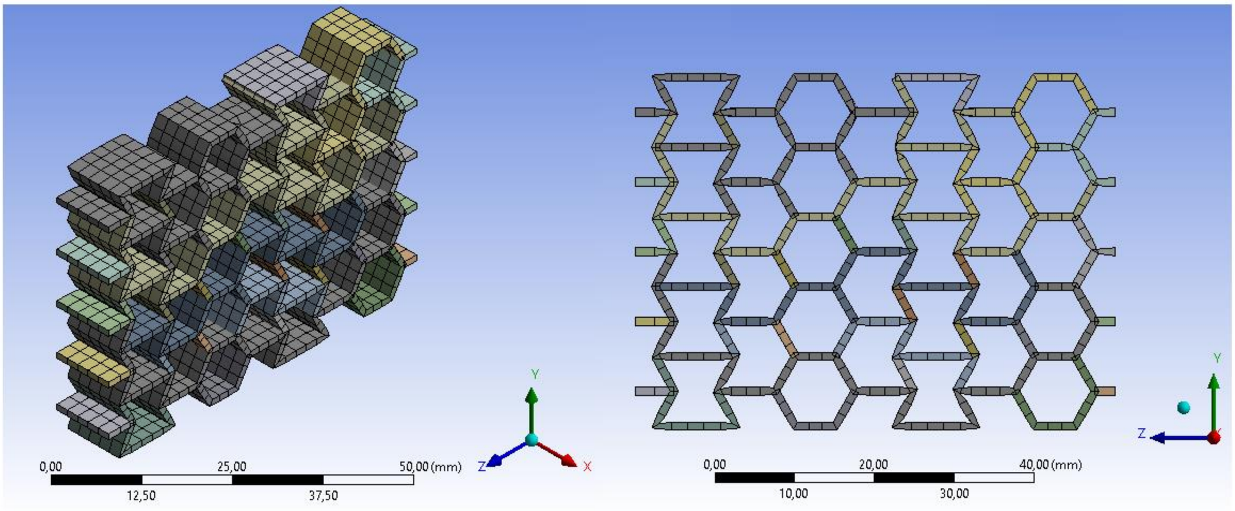

Figure 7 – Frontal and isometric views of model meshing used for simulation of shell elements (surfaces).

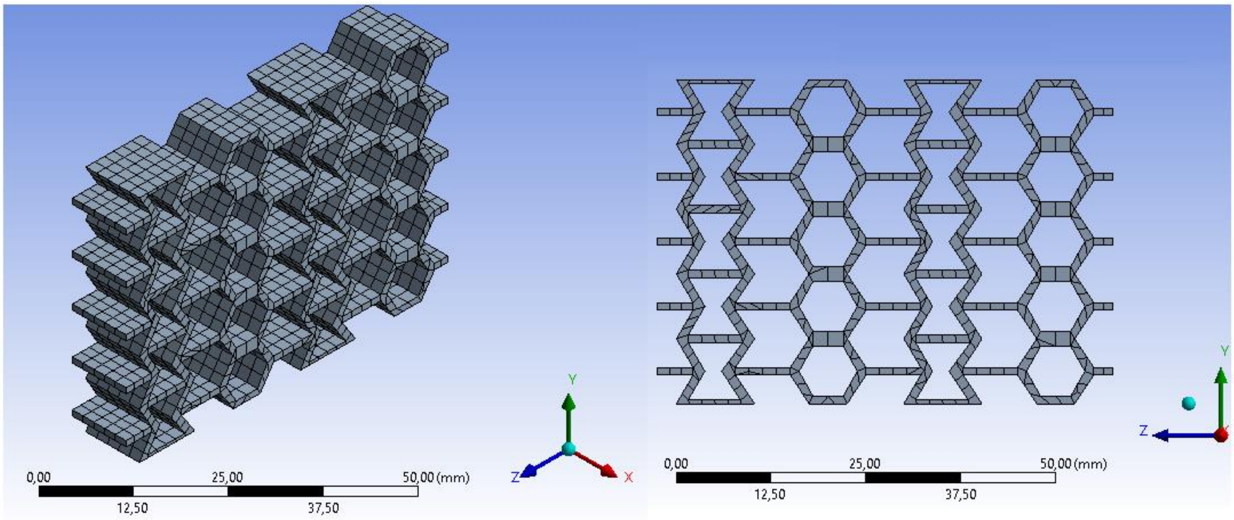

Figure 8 – Frontal and isometric views of model meshing used for simulation of three-dimensional elements (solid body).

2.4 Models Constraints

For each model, two different simulations were performed. The difference from one situation to the other was in the imposition of constraints. In the first situation, the four lower faces (of the base) on the *Y*-axis were applied a fixed constraint (fully constrained base), while the five rods on the right side were constrained in relation to the horizontal displacement, this means a null displacement along *Z*-axis. The four upper surfaces were submitted at a constant negative vertical displacement (*Y*-axis) of 1mm. This situation can be schematically seen in Figure 9.

The second situation presents a fixed constraint (restriction of all degrees of freedom) on the five rods on the right side, while the four faces of the base have a constraint to displacement along the vertical *Y*-axis (zero displacement) and, finally, a compression displacement of 1mm was imposed along *Z*-axis on the five rods on the left side. Such situation can be schematically seen in Figure 10.

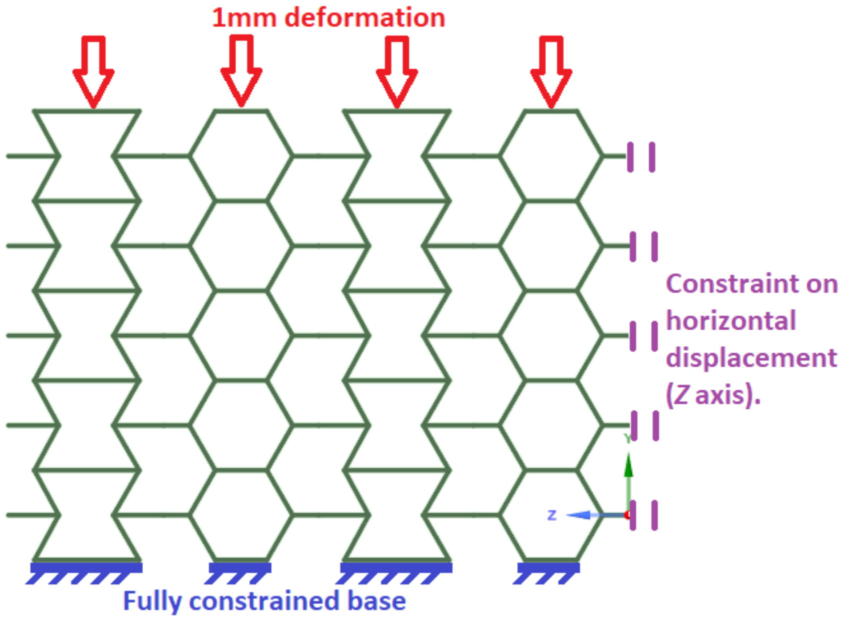

Figure 9 – Constraints of the first situation used for finite element simulations of beam, shell and body models (1mm compression displacement along *Y*-axis).

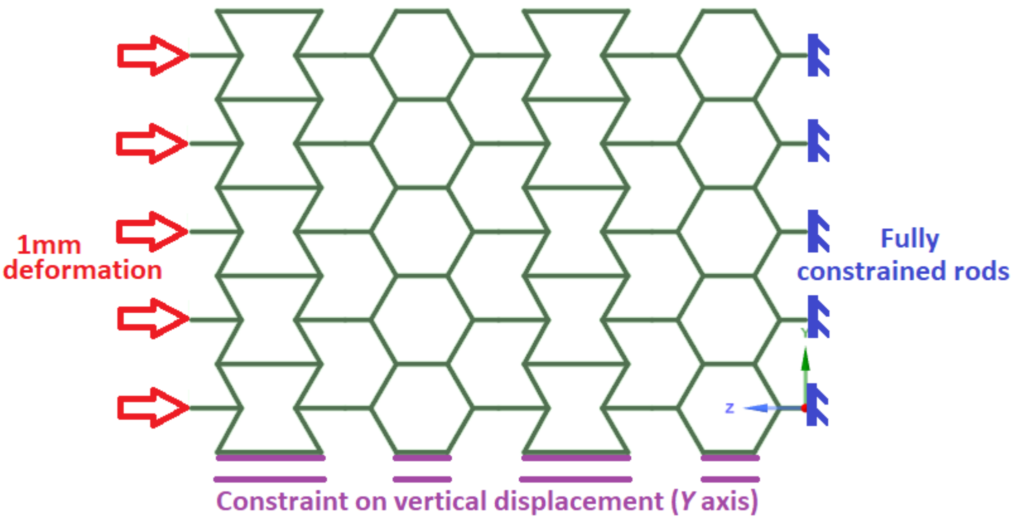

Figure 10 – Constraints of the second situation used for finite element simulations of beam, shell and body models (1mm compression displacement along *Z*-axis).

3. Results and discussions

The total deformation profiles of each simulation were generated in order to verify if there were significant differences in values when performing the three different types of modeling. First, it is worth mentioning that the computational time of simulations increases as the dimension of the elements increases; less computational time was spent using beam elements, then intermediate time was spent using two-dimensional elements (shell) and finally more time was spent using three-dimensional elements. Solid element modeling is able to more faithfully represent the geometry and constraints of an experimental structure, however, one-dimensional and two-dimensional elements might also lead to results close to volumetric modeling, with the advantage of lower computational cost.

Furthermore, two situations were imposed since the geometry is not regular comparing the two vertical and horizontal axes, *Y* and *Z*, respectively, which may lead to different mechanical responses even if the same fixed compression displacement in the both directions is imposed. This is why two simulations were performed for each of the three models.

Thus, the two followed subtopics present the results obtained after the simulations, showing the total deformation profiles.

3.1 Compression Along Y-axis (Vertical)

On Figures 11, 12 and 13 it is possible to see the front view of total deformation profiles of beam, shell and body modeling, respectively, when applying a compression displacement of 1mm along *Y*-axis.

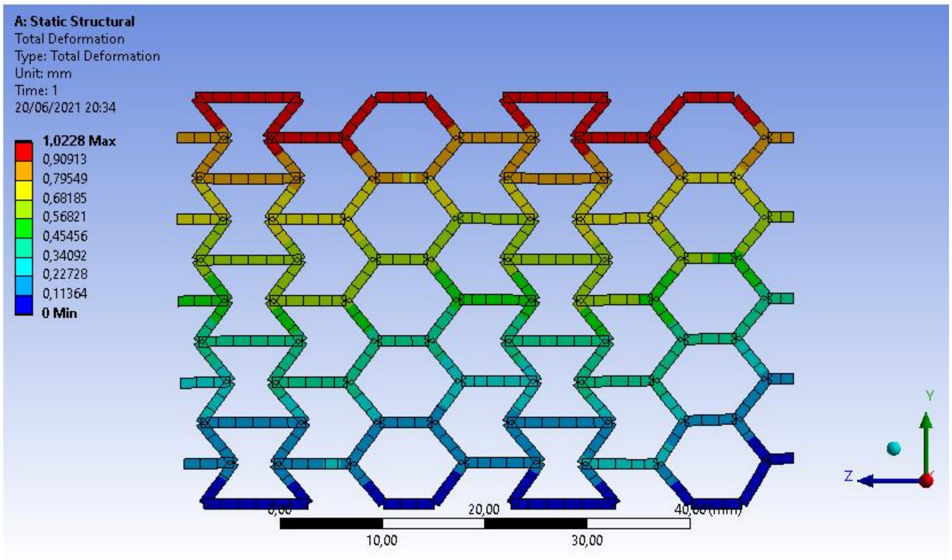

Figure 11 – Front view of total deformation profile of each element in beam element simulation when applying a vertical compression displacement of 1mm.

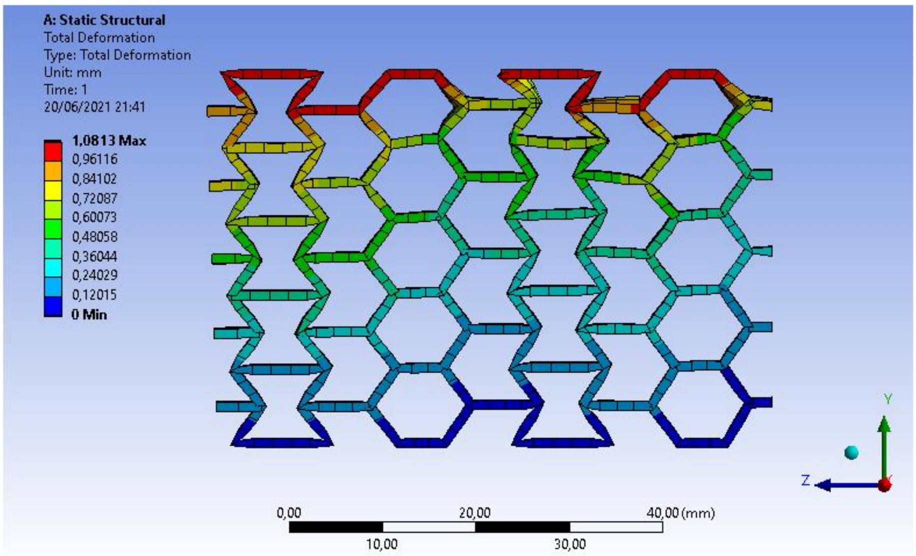

Figure 12 – Front view of total deformation profile of each element in shell element simulation when applying a vertical compression displacement of 1mm.

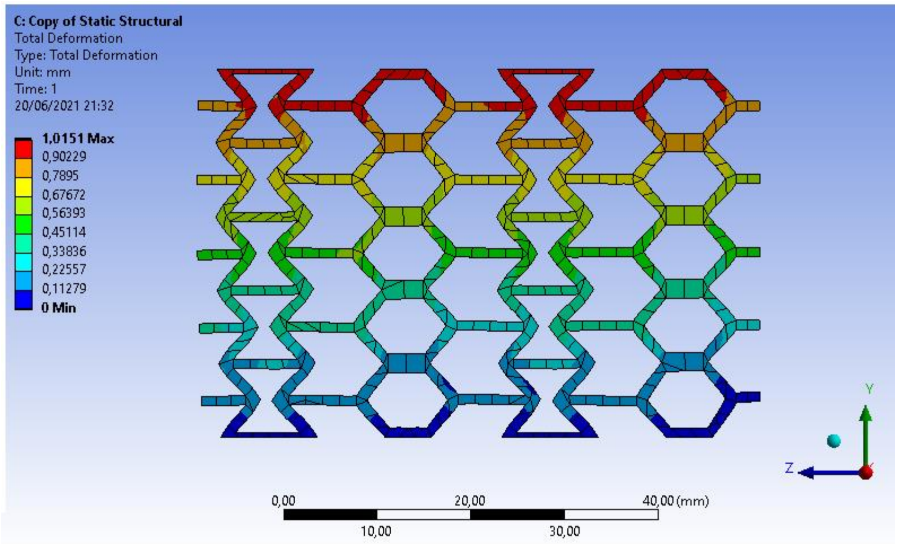

Figure 13 – Front view of total deformation profile of each element in body element simulation when applying a vertical compression displacement of 1mm.

It is possible to note that, for the three models, the total deformation profiles are quite similar. The advantage of this is that it is possible to use shell or beam elements to obtain a faster and reliable result in simulations of greater structures, in which the computational cost is a relevant issue. For this set of constraints, the maximum total deformation of beam, shell and solid modeling were, respectively: 1.0228mm, 1.0813mm and 1.0151mm. In this case, the beam modeling showed numerical value closer to the result obtained from three-dimensional element, which was 0.75% higher. On the other hand, shell modeling presented a value 6.5% greater than the value obtained by solid modeling. This difference may have occurred because the union of surfaces in shell modeling might not have been perfect, even though they are adequate and similar results to solid modeling.

The stress profiles were also qualitatively evaluated for the three models and it was possible to see the same pattern for the three modeling and it is observed highest stresses in the structure vertices. This shows, once again, that it is possible to obtain adequate results also with shell and beam modeling.

3.2 Compression Along Z-axis (Horizontal)

On Figures 14, 15 and 16 it is possible to see the front view of total deformation profiles of beam, shell and body modeling, respectively, when applying a compression displacement of 1mm along *Z*-axis.

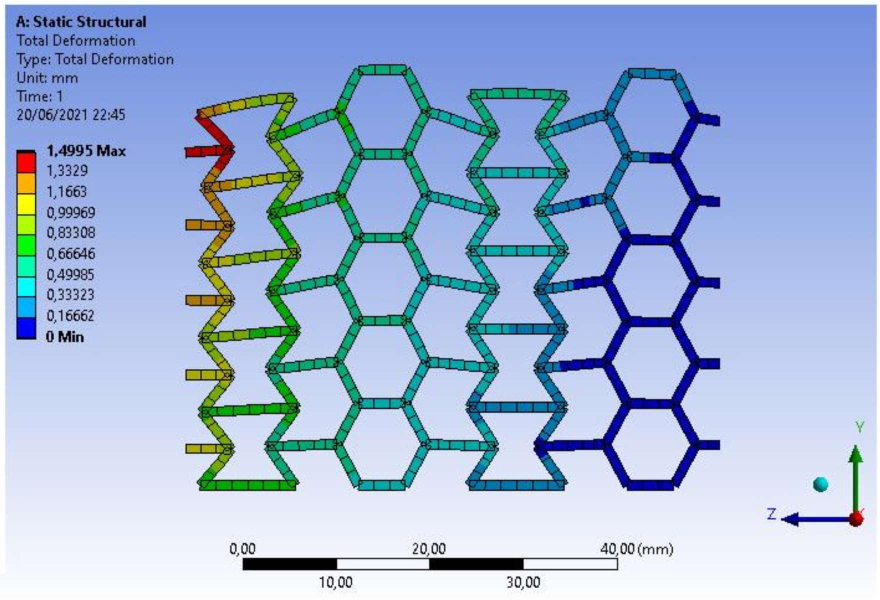

Figure 14 – Front view of total deformation profile of each element in beam element simulation when applying a horizontal compression displacement of 1mm.

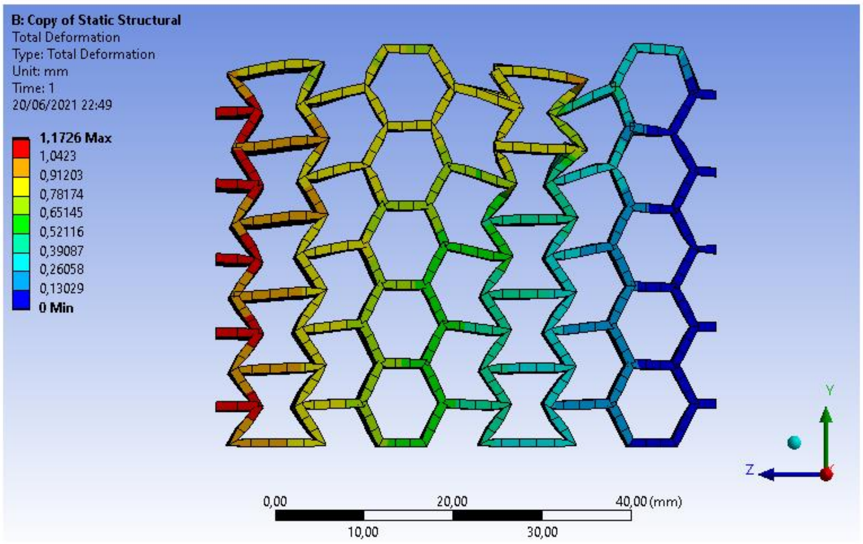

Figure 15 – Front view of total deformation profile of each element in shell element simulation when applying a horizontal compression displacement of 1mm.

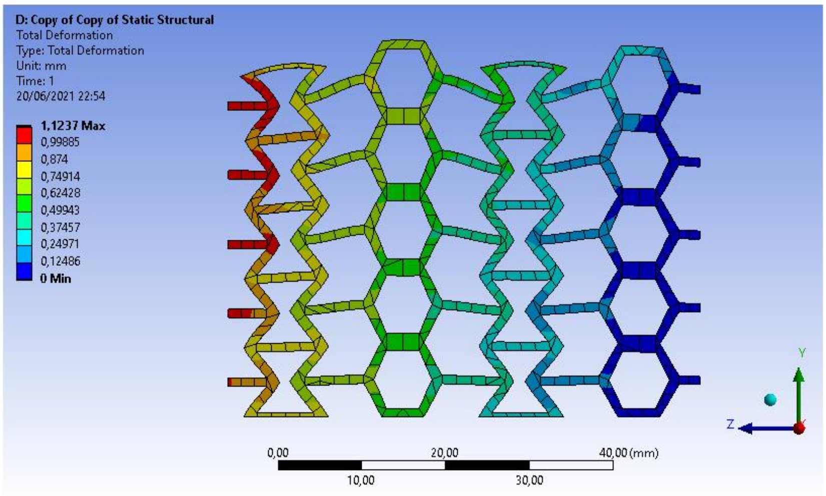

Figure 16 – Front view of total deformation profile of each element in body element simulation when applying a horizontal compression displacement of 1mm.

Once again, the three models showed similar total deformation profiles. However, for this set of constraints, shell modeling presented results closer to solid modeling than beam element. The maximum total deformation of beam, shell and solid modeling were, respectively, 1.4495mm, 1.1726mm and 1.1237mm. This means that the value of shell modeling was 4.3% higher than the value obtained by solid modeling and the value obtained by beam modeling was 29% higher. For this case, the values of beam modeling were significantly higher than the solid modeling, thus evincing that the use of beam element is not adequate for this set of constraints. This may have occurred because, when restricting the displacement in relation to *Y*-axis of the elements from the structure base, as the elements are one-dimensional, the displacement in the *X*-axis also remains restricted by consequence, while in the cases of shell and solid elements, the vertical movement of the base is restricted, but the displacement along *X*-axis remains possible.

Finally, the stress profiles of the three models were also qualitatively analyzed and it was also possible to observe that a concentrated stress is at the vertices of structure's geometries.

4. Conclusions

The objectives of this work were achieved in which consisted to compare the results obtained by finite element simulations applying two sets of constraints in unidirectional fibrous composite metamaterial structures of re-entrant auxetic geometry combined with honeycomb geometry using three distinct finite element modeling: beam, shell and solid.

When applying a vertical compression displacement of 1mm, the maximum total deformation values of beam, shell and solid models were, respectively: 1.0228mm, 1.0813mm and 1.0151mm, which means the value obtained using beam element was 0.75% higher than the result of the solid modeling, while the result of shell element was 6.5% higher. On the other hand, when applying a compression displacement along the horizontal axis, the results of the maximum values of total deformation of beam, shell and solid models were, respectively, 1.4495mm, 1.1726mm and 1.1237mm. This means that the beam simulation leads to a value 29% higher than the solid modeling, while the shell simulation leads to a 4.3% higher result. Therefore, it is concluded that, for the presented structure, the shell modeling displays an adequate approximation to the three-dimensional model, being able to be applied in cases of similar simulations, while the modeling with beam elements did not show accurate results. The advantage of using a shell element (two-dimensional) in detriment of a three-dimensional element is the lower computational cost.

Finally, in order to validate simulation results, it would be interesting to carry out experiments with the same setup. Therefore, it is expected that this work can be used as an inspiration for the fabrication of prototypes of this structure made of composite material, preferably using the additive manufacturing process commonly called as 3D printing.

References

Chen, Z., Yan, N., Deng, J., & Smith, G. (2011). Flexural creep behavior of sandwich panels containing Kraft paper honeycomb core and wood composite skins. *Materials Science and Engineering: A*, 528(16-17), 5621-5626. doi: https://doi.org/10.1016/j.msea.2011.03.092

Crupi, V., Epasto, G., & Guglielmino, E. (2012). Collapse modes in aluminium honeycomb sandwich panels under bending and impact loading. *International Journal of Impact Engineering*, 43, 6-15. doi: http://dx.doi.org/10.1016/j.ijimpeng.2011.12.002

Daniel, I. M., & Ishai, O. (2006). *Engineering Mechanics of Composite Materials*. Oxford University.

Fei, X., Jin, L., Zhang, X., Li, X., & Lu, M. (2020). Three-dimensional anti-chiral auxetic metamaterial with tunable phononic bandgap. *Applied Physics Letters*, 116(2), 021902. doi: http://dx.doi.org/10.1063/1.5132589

Jones, R. M. (1990). *Mechanics of Composite Materials*. Taylor & Francis, Inc.

Karathanasopoulos, N., Dos Reis, F., Reda, H., & Ganghoffer, J.-F. (2018). Computing the effective bulk and normal to shear properties of common two-dimensional architectured materials. *Computational Materials Science*, 154, 284-294. doi: http://dx.doi.org/10.1016/j.commatsci.2018.07.044

Masters, I. G., & Evans, K. E. (1996). Models for the elastic deformation of honeycombs. *Composite Structures*, 35(4), 403-422. doi: http://dx.doi.org/10.1016/s0263-8223(96)00054-2

Mousanezhad, D., Haghpanah, B., Ghosh, R., Hamouda, A. M., Nayeb-Hashemi, H., & Vaziri, A. (2016). Elastic properties of chiral, anti-chiral, and hierarchical honeycombs: a simple energy-based approach. *Theoretical and Applied Mechanics Letters*, 6(2), 81-96. doi: http://dx.doi.org/10.1016/j.taml.2016.02.004

Shruti, M., Hemanth, N. S., Badgayan, N. D., & Sahu, S. K. (2021). Compressive behavior of auxetic structural metamaterial for lightweight construction using ANSYS static structural analysis. *Materials Today: Proceedings*, 38, 12-17. doi: http://dx.doi.org/10.1016/j.matpr.2020.05.410

Wang, H., Lu, Z., Yang, Z., & Li, X. (2019). A novel re-entrant auxetic honeycomb with enhanced in-plane impact resistance. *Composite Structures*, 208, 758-770. doi: http://dx.doi.org/10.1016/j.compstruct.2018.10.024

Wang, T., Wang, L., Ma, Z., Hulbert, & G. M. (2018). Elastic analysis of auxetic cellular structure consisting of re-entrant hexagonal cells using a strain-based expansion homogenization method. *Materials & Design*, 160, 284-293. doi: http://dx.doi.org/10.1016/j.matdes.2018.09.013

Xu, M., Xu, Z., Zhang, Z., Lei, H., Bai, Y., & Fang, D. (2019). Mechanical properties and energy absorption capability of AuxHex structure under in-plane compression: theoretical and experimental studies. *International Journal of Mechanical Sciences*, 159, 43-57. doi: http://dx.doi.org/10.1016/j.ijmecsci.2019.05.044

Zhong, R., Fu, M., Yin, Q., Xu, O., & Hu, L. (2019). Special characteristics of tetrachiral honeycombs under large deformation. *International Journal of Solids and Structures*, 169, 166-176. doi: http://dx.doi.org/10.1016/j.ijsolstr.2019.04.020